Combustion Characteristics of HAN-based Green Propellant Assisted with Nanoporous Active Carbons

M.K. Atamanov[1,2*], R. Amrousse[3,4], J. Jandosov[1,2], K. Hori[4], A.R. Kerimkulova[1,2], D.I. Chenchik[1], B.Y. Kolesnikov[1]

[1]Institute of Combustion Problems, Bogenbay batyr ave. 172, Almaty, Kazakhstan
[2]al-Farabi Kazakh National University, al-Farabi ave. 71, 050040 Almaty, Kazakhstan
[3]University of Chouaïb Doukkali, Faculty of Sciences, 24000 El Jadida, Morocco
[4]ISAS/JAXA, Japan Aerospace Exploration Agency, 3-1-1 Yoshinodai Chuo-ku, Sagamihara 252-5210, Kanagawa, Japan

Article info

Abstract

Combustion of hydroxylammonium nitrate (95 wt.% HAN) – water solution in presence of high specific surface area activated carbons is investigated in a constant-pressure bomb within the pressure range of 1–6 MPa. The linear burning rate increased for the system of HAN admixed with activated carbons compared to those of the HAN alone. Moreover, the thermal decomposition of HAN (95 wt.%) – water solution spiked with activated carbons was assessed by DTA – TG method. In the presence of activated carbons, the ability to trigger the decomposition at a lower temperature (86 °C vs 185 °C) was observed. The volatile products formed in the course of thermal decomposition of HAN, spiked with activated carbons were characterized by electron ionization mass spectrometry analysis. Primary products of HAN decomposition: $m/z = 33$ (NH_2OH) and $m/z = 63$ (HNO_3), which are further responsible for the formation of secondary products such as N_2O, NO, HNO_2, NO_2, O_2 etc. Significant reduction of NOx emissions during thermal decomposition of HAN (95 wt.%) – water solution was observed (ca. 30%) in presence of activated carbons.

1. Introduction

In the aerospace industry, hydrazine is the most used propellant in the satellite control systems. Widely applicable catalyst for the monopropellants is iridium metal, which as known as very expensive. Unfortunately, propellants based on hydrazine considered extremely toxic. Therefore, by the end of the twentieth century, the research centers have an intention on searching of new less harmful and higher-energy materials. Aqueous compounds such as hydroxymammonium nitrate (NH_3OHNO_3) were proposed as one of the most promising alternative for hydrazine [1–2].

This material is less toxic, has a high density and production, predominating the most energy-intensive materials, it is used and considered as the primary oxidant for hybrid rockets. Due to exten-sive studies, we can summarize that the combustion of HAN is subjected to the influence of initial pressure [3–5].

However, for a wide range of HAN there is existed a number of obstacles, such as the necessity of high temperature for decomposition beginning and low burning rate etc. Therefore, the catalytic additives from platinum group, as well as nanoparticles such as Al and SiO_2 were used for the effective application [6]. The activated carbons with a high-surface area based on rice husk were investigated as a perspective additive in this work [7]. Rice husk is a large-scale vegetable unique material, e.g.: it is renewable, green material with low commercial value [8]. The main purpose of this research is the comprehensive study of combustion behavior of HAN as a green alternative in the presence of different activated carbons with high specific surface area (SSA) (up to 3000 m^2/g).

---

*Corresponding author. E-mail: amk1310@mail.ru

The paper consists of three main research tasks: (i) Experimental studies of activated carbons influence on the linear burning rates HAN-based propellant in high-pressure chamber; (ii) Kinetic analysis of thermal decomposition HAN-based propellant is supplied by activated carbon with high SSA by DTA-TG analysis; (iii) EI-MS analysis of HAN thermal decomposition is admixed with different types of activated carbon for understanding of carbon influence on the behavior of investigated object.

2. Materials and Methods of Investigation

2.1. Activated carbon

In this work, we used the activated carbons (CRH-K_2CO_3, CRH-KOH and CRH-H_3PO_4) with high surface area is derived from carbonised rice husk (CRH). Materials were obtained by carbonisation of rice husk at different high temperature pyrolysis in inert argon atmosphere followed by chemical activation with active chemical reagents such as K_2CO_3, KOH or H_3PO_4. These activated carbons were obtained in the Laboratory of Carbon Nanomaterials and Nanobiotechnology of the Institute of Combustion Problems (Almaty, Kazakhstan).
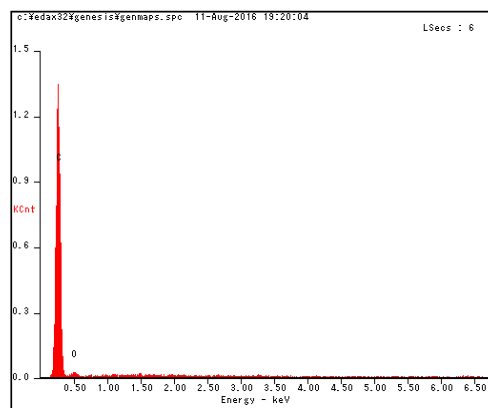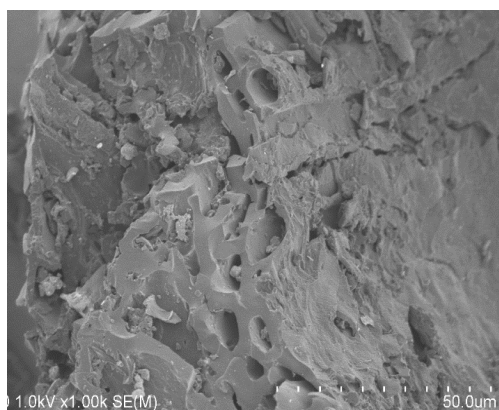
Also for comparison, we used the commercial activated carbon "AC-RF" from OJSC "Irbitsky Chemical and Pharmaceutical Plant", Russian Federation, registration number is: № RK-LS-5N006618.

As an example, the characteristic of morphology and elemental analysis for one of used material (activated carbon CRH-KOH) shown in Fig. 1. The surface area and adsorption capacity for all four activated carbons is shown in Table 1.

Table 1

Adsorption capacity of activated carbon samples by methylene blue with water
(according to GOST 4453-74) and the BET specific surface area (S_{BET})

Activated carbon	Samples weight, g	Initial concentration of the indicator, mg/dm^3	Optical density, D	Volume of indicator solution, dm^3	Transmittance capacity, T%	Adsorption capacity, mg/g	S_{BET}, m^2/g
KOH	0.1	1500	0.062	0.025	96.6	372	2926
K_2CO_3	0.1	1500	0.031	0.025	95	370	900
H_3PO_4	0.1	1500	0.504	0.025	87.8	365	1220
AC-RF	0.1	1500	0.479	0.025	22.9	268	410

Element	Wt%	At%
CK	91.98	93.85
OK	8.02	6.15
Matrix	Correction	ZAF

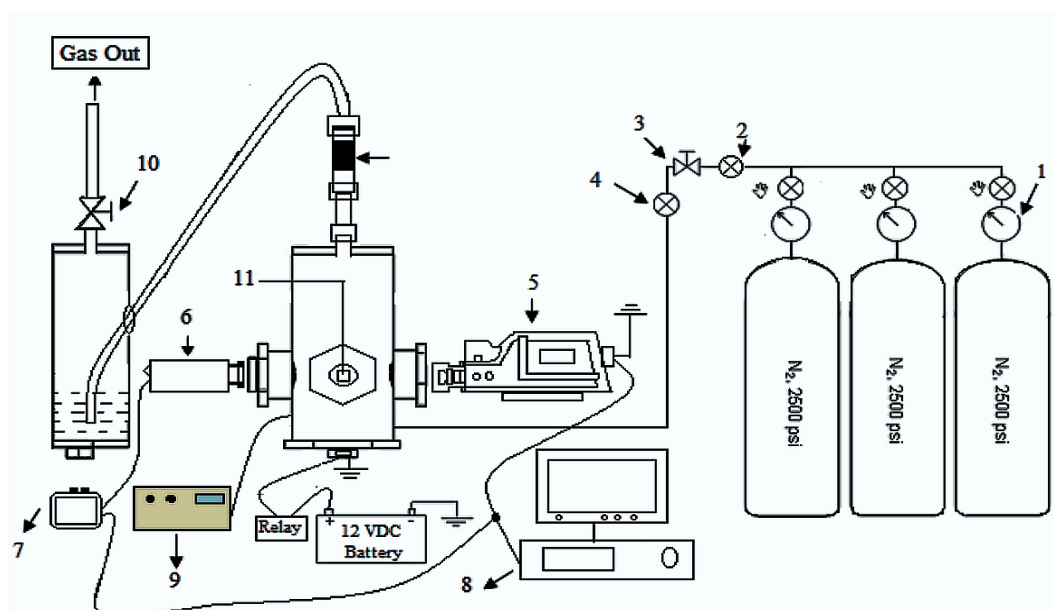Fig. 1. SEM and EDAX analysis of activated carbon CRH-KOH.

Fig. 2. Scheme of an enclosed bomb to testing of burning rate: 1 – manometer; 2 – community manometer; 3 – reduction gear; 4 – manometer of pressure inside of chamber; 5 – high-speed camera; 6 – the chamber; 7 – the monitor; 8 – the PC; 9 – pressure sensor; 10 – output of exhaust gases; 11 – source of artificial light;

2.2. Burning test

In order to investigate the linear burning rate, there is used a high-pressure chamber where the samples are subjected to gas pressure N_2. The ignition delay, initial pressures and combustion process are recorded by Lab-view software (NI USB-6229) with the sampling rate of 1000 Hz have been investigated. The accuracy of pressure sensor is ± 0.5% FSO (Full l Scale Output) and equal to 0.076 MPa. The high-pressure camera is equipped with a high-speed camera "PHOTRON" with settings of 1000 frames per second and a resolution of 640X488. The experiments on combustion of HAN with activated carbon were carried out in high-pressure chamber by ignition with electric power at constant pressure from 1–6 MPa. The samples with weight of 2 g, in height of 10 mm and in diameter of 6 mm were placed into the high-pressure chamber as shown in Fig. 2.

2.3. The differential thermal analysis

The kinetic studies were carried out by DTA-TG analysis. In this work we used a modulated DTA device "RIGAKU TG8120-TG-DTA", operating in the temperature range from -180 to +725 °C with an accuracy of ± 0.05 °C and a heating rate of 0.1–25 °C/min with a working weighing up to 200 mg with vertical loading of samples. To exclude the effect of air on the resulting thermograms, the studies were carried out in nitrogen media (N_2 – 100 cm^3/min). Samples were placed in aluminum crucibles with vertical loading. The DTA-TG analysis allows to obtain the following information: (a) initial temperatures; (b) evaporation points (endothermic peak); (c) decomposition temperature is conditioned by the inflexion point of temperature curve; d) mass loss etc. [9].

2.4. Electron Ionization – Mass Spectrometry (EI-MS) analysis

The electron ionization (EI) spectra were investigated using TSQ 700 mass spectrometer with an adjustable heating rate of samples. The electron energy was 70 eV and the emission current was 200 mA. The temperature of ion sources was 150 °C, and the scanning range was $m/z = 0–200$. Trace amounts of test samples were loaded into aluminum crucibles (SUS) and inserted directly into the source. The probe temperature was increased from 25 °C to 600 °C at different heating rates varied from 16; 32; 64 and 128 K/min.

3. Results and discussion

3.1. The combustion experiments in strand burner

We analyzed the effect of different types of activated carbon on the combustion performance of HAN (95 wt.%) – water solution. The linear burning rates of the HAN-based propellant admixed with activated carbon are monitored and recorded by

the high-speed camera. The experiments of HAN combustion were carried out in liquid phase and at different initial starting pressures. According to the obtained results, initial pressures and additive concentration have influenced on the burning rate and ignition characteristics.

Figure 3 shows a comparative result of the linear burning rate of HAN (95 wt.%) – water solution, depending on different values of initial pressure and various additives with activated carbon (AU-RF, CRH-K$_2$CO$_3$, CRH-KOH, CRH-H$_3$PO$_4$) at a ratio of 99% – HAN and 1% of activated carbon.

The results of this work are compared with working results of B.N. Kondrikov et al. [10], who were used a similar experimental setup. The highest burning rate result was achieved in the presence of activated carbon "CRH-KOH". Each additive of activated carbon is provided a significant enhancement of HAN burning rate. The samples of activated carbon CRH-K$_2$CO$_3$ and AC-RF had shown approximately small effect of HAN combustion character, but despite this, the burning rate is increased about 9 times at initial pressure of 6 MPa compared with HAN alone. Therefore, there is a question concerning the role of activated carbon on combustion mechanism of HAN. The combustion of HAN may be enhanced due to reduction of decomposition temperature of intermediate reactions. It should be noted that the combustion character of these systems is completely different from the studied compositions with high concentration of water in HAN aqueous solutions [11, 12]. As a result, they assumed that the high burning rate is caused by water boiling as well as the high reaction rate, and may be associated with the hydrodynamic
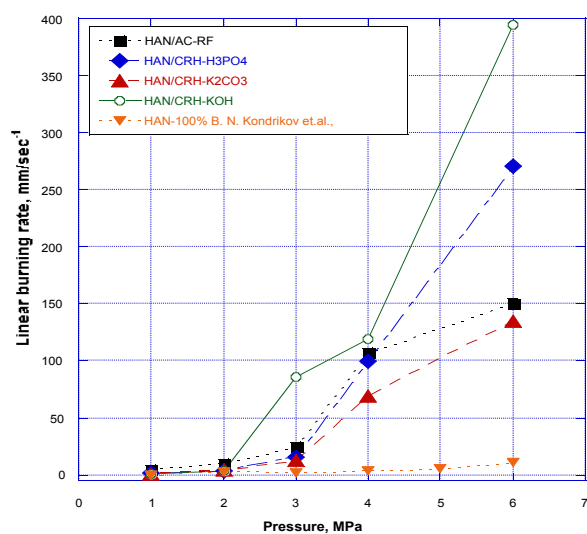
instability mechanism, which is described by the Landau-Levich theory, is suitable for liquid rocket propellants.

It is known that the concentration of additives such as (catalysts, promoters, inhibitors, etc.) influencing on burning rate of energy-intensive compositions, is related to an increase of reactants number during the chemical reaction. The effect of activated carbon concentration on burning rate of HAN (95 wt.%) – water solution is shown in Fig. 4.

Figure 4 shows the measurements results of the linear burning rate of HAN at 4 MPa an initial pressure in the different concentration of activated carbon CRH-KOH. According to the curve, the obtained graph shows the rising of activated carbon concentration in order to reach the burning rate in four times. The slope can be described by the following equation:

$$r_A = k\,[A]^2$$

where r_A – is the reaction rate depending on the concentration of reagents; $[A]$ – is the concentration of the substance, k – is the reaction rate constant. Such noticeable increase of burning rate is associated with good activity and high specific surface area from activated carbon CRH-KOH, which is almost 3000 m^2/g. The surface and the edges of activated carbon have many defects, which can act as a matrix for the formation and stabilization of free radicals (OH radicals) [13], which are formed during the decomposition of nitric acid, is described in following reaction and were proposed by T.B. Brill, and Y.J. Lee [14, 15]:
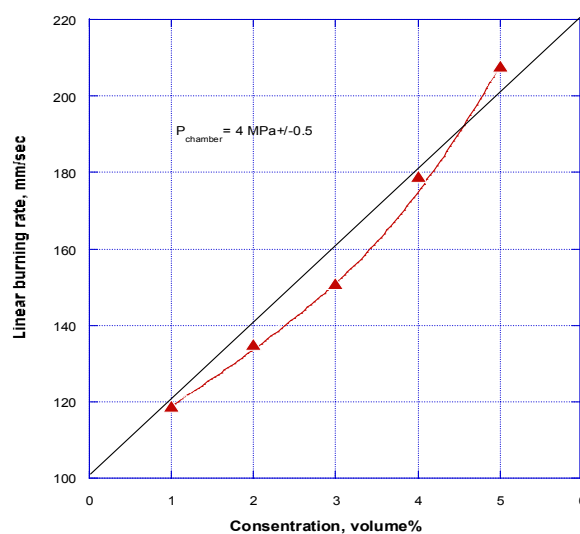
$$HNO_3 \rightarrow NO_2 + OH \qquad (1)$$

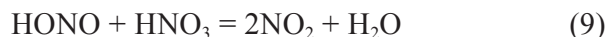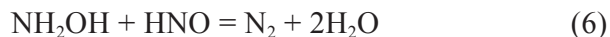Fig. 3. The Effect of activated carbons additives on the burning rate of HAN (95 wt.%) – water solution.

Fig. 4. Effect of activated carbon CRH-KOH concentration on burning rate of HAN (95 wt.%) – water solution.

3.2. Experimental studies of Thermal analysis of decomposition HAN with carbonized rice husk by DTA-TG

The decomposition of HAN (95 wt.%) – water solution in the presence of iridium catalyst or activated carbon (CRH-KOH) has been carried out and an example of DTA-TGA comparable results are presented in Fig. 5.

The DTA curve shows the exothermic phenomena only as a strong peaks at the presence of additives and large endothermic peak with conversion into the soft exothermic peak in pure HAN (95 wt.%) – water solution. According to the literature data [16, 17] the mechanism of thermal decomposition of HAN is described with following main reactions.

$$HAN + H_2O = NH_2OH + HNO_3 + H_2O \quad (2)$$

$$NH_2OH + HNO_3 = HONO + HNO + H_2O \quad (3)$$

$$NH_2OH + HONO = N_2O + 2H_2O \quad (4)$$

$$2HNO = N_2O + H_2O \quad (5)$$

$$NH_2OH + HNO = N_2 + 2H_2O \quad (6)$$

$$3HONO = 2NO + HNO_3 + H_2O \quad (7)$$

$$HNO + HNO_3 = 2HONO \quad (8)$$

$$HONO + HNO_3 = 2NO_2 + H_2O \quad (9)$$

Iridium catalyst has presented the catalytic activity toward the HAN decomposition reaction which is evidenced by the exothermic peaks presence; the exothermic peak profile depends obviously on activated phase of the catalyst. The decomposition of HAN is occurred at a temperature which is higher than 74.3 °C, but the maximum temperature is 151.6 °C. As can be seen from the DTA curve (90HAN/10Ir), the obtained results consistent with previously described process of catalytic decomposition of HAN water solutions [1, 16, 17].

Also, there is observed a close similarity in the thermal decomposition of HAN (95 wt.%) – water solution admixed with 10% of activated carbon CRH-KOH (90HAN/10CRH-KOH). The decomposition has been started around 86 °C and has highly exothermic reaction with a maximum
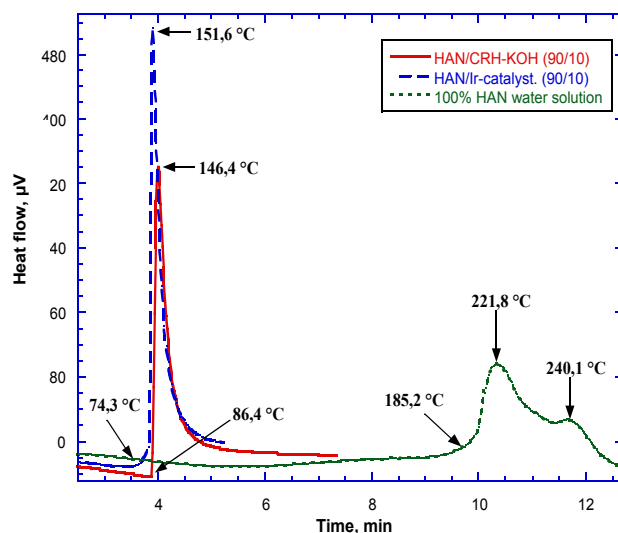

Fig. 5. DTA-TGA curves of the thermal decomposition of HAN (95 wt.%) – water solution in the presence of Ir catalysts and activated carbon CRH-KOH at 20 K/min heating rate.

at 146.4 °C. The results of HAN – water solution decomposition admixed with activated carbon is very close to the results of HAN – water solution decomposition in presence of iridium catalyst.

Decomposition of HAN (95 wt.%) – water mixture in the presence of four types of activated carbon (CRH-K$_2$CO$_3$, CRH-KOH, CRH-H$_3$PO$_4$ and AC-RF) in the mode of temperature increase was investigated at heating rate of 20 K/min; the results are presented in Fig. 6.

Figure 6 shows the temperature profile with the highest temperatures of exothermic reaction during decomposition of HAN (95 wt.%) – water solution with 1% of concentration of various activated carbons (CRH-K$_2$CO$_3$, CRH-KOH, CRH-H$_3$PO$_4$ and AC-RF). Basically, the high energy release at HAN decomposition with activated carbons carbons (CRH-K$_2$CO$_3$, CRH-KOH, CRH-H$_3$PO$_4$) is occurred by one steps is observed between 90–300 °C. But, the decomposition of HAN/AC-RF mixture with is occurred with exotherm of two peaks at 209 and 288 °C. This phenomenon has been noted in the previous studies [1, 2, 17] concerning the decomposition of HAN without any additives, where a two-stage mechanism for decomposition of the mixture is proposed. Thus, we guess that activated carbon AC-RF, does not change the decomposition mechanism of HAN. The activated carbon sample CRH-H$_3$PO$_4$,T has shown the highest exothermic maximum at 274 °C which is higher on 50 °C and at the same time is faster than the pure mixture of HAN.
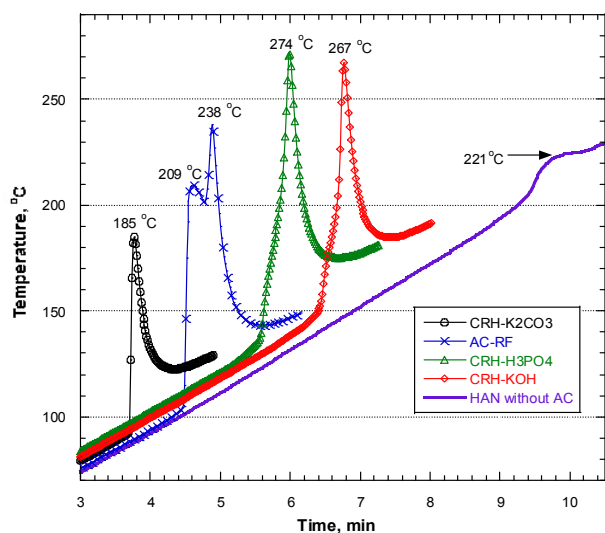
Fig. 6. The temperature profile as a function of time for decomposition of HAN (95 wt.%) – water solution in presence of activated carbon CRH-K$_2$CO$_3$, CRH-KOH, CRH-H$_3$PO$_4$ and AC-RF at 20 K/min heating rate.

Effect of all activated carbons is demonstrated by thermal analysis showed a perspective results. In accordance with the DTA-TG profiles, the HAN decomposition reaction is occurred very fast with realization of high temperature, high decomposition rate, and heat release during the decomposition.

3.3. The results of Electron Ionization – Mass spectrometry

Electron Ionization – is the mass spectrometry analysis (EI-MS) of thermal decomposition of pure (Fig. 7a) HAN (95 wt.%) – water solution and (Fig. 7b) HAN (95 wt.%) – water solution in presence of 1~3 wt.% activated carbon CRH-KOH were carried out in Fig. 7.

The MS results corresponding to the decrease of peak intensity $m/z = 30$ (NO) during introduction of activated carbon. The availability of peaks O$_2$/N$_2$O and NO ($m/z = 32$ and 44, 30) in MS, a high reaction rate and low temperature range may prove the absence of CO and CO$_2$ in decomposition reaction of HAN [18, 19]. At decomposition of HAN with activated carbon KOH, there is observed the phenomenon of N$_2$O and NO$_2$ ions decreasing. This may be associated with short time scales and low reaction temperature is described by Ya.B. Zel'dovich et al. [20].

The EI-MS analyses of thermal decomposition of pure HAN (95 wt.%) – water solution and HAN (95 wt.%) – water solution in the presence of 1~3 wt.% of activated carbon CRH-KOH and corresponding

ion current depends on temperature and time of ion fragments during thermal decomposition is given in Fig. 8a and b respectively.

MS detects the primary products of HAN decomposition in the range from $m/z = 29$–300 where: $m/z = 33$ (NH$_2$OH) and $m/z = 63$ (HNO$_3$) are observed, which are responsible for the formation of secondary ions such as NO, OH, HONO, N$_2$O, NO$_2$ and etc. The study results are corresponding to the work data of H.S. Lee and T.A. Litzinger [21]. The graph shows the total recorded masses from formation of peaks: $m/z = 32$ (O$_2$), $m/z = 44$ (N$_2$O) and $m/z = 46$ (NO$_2$). Pure HAN has decomposes by two stages: low temperature decomposition (LTD) and high temperature decomposition (HTD) [22]. The first stage starting at 100 °C with the formation of NH$_2$OH, NO, NO$_2$ and HNO$_3$ ions and ended at 150 °C. At the second stage there is observed the formation of N$_2$O and continuous formation of NO ions up to 300 °C. Activated carbon in ratio of 1~3 wt.% is promoted to the double-stage decomposition of pure HAN and it becomes single-stage at 220–290 °C with reduction of decomposition temperature by 40–45 °C in accordance with DTA-TG results.
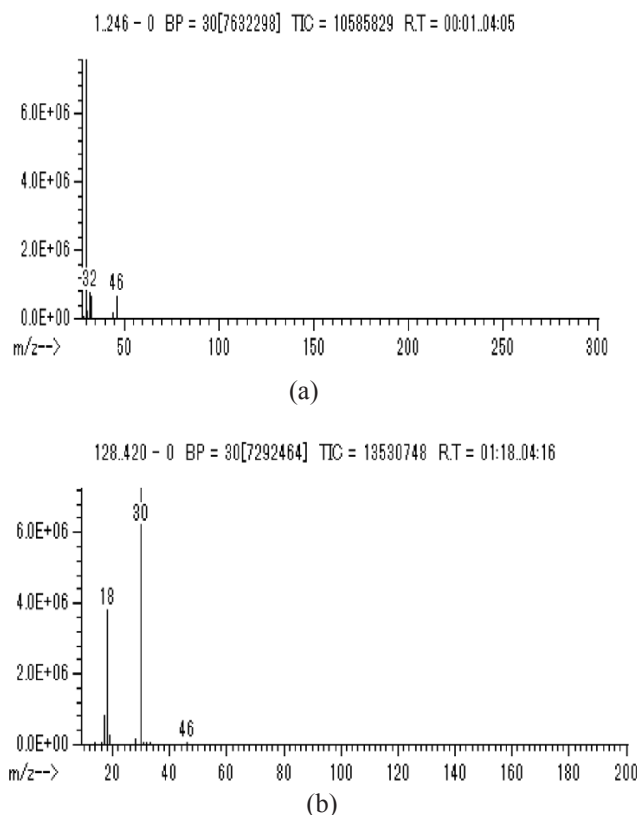

(a)

(b)

Fig. 7. Comparison of mass spectrum at thermal decomposition of (a) pure HAN (95 wt.%) – water solution versus (b) HAN (95 wt.%) – water solution admixed with activated carbon CRH-KOH is provided by EI-MS analysis.
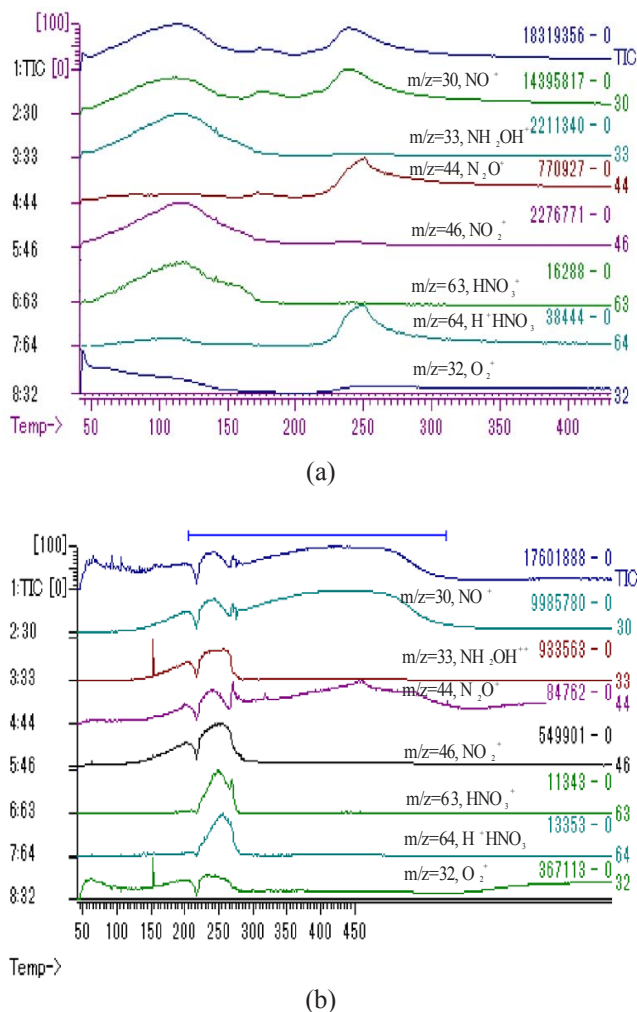
(a)

(b)

Fig. 8. Ion current temperature curves of ion fragments during the thermal decomposition of (a) pure HAN (95 wt.%) – water solution versus (b) HAN (95 wt.%) – water solution spiked with activated carbon CRH-KOH provided by EI-MS analysis.
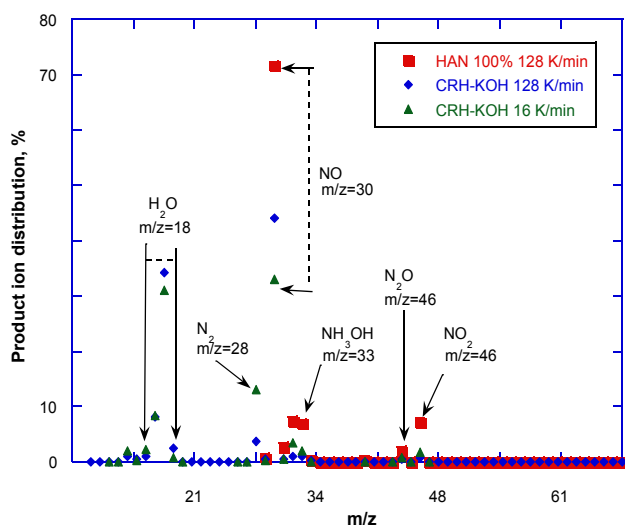

Fig. 9. Comparison of product ion distribution of pure HAN (95 wt.%) – water solution versus HAN (95 wt.%) – water solution admixed with activated carbon CRH-KOH at different heating rates (16–128 K/min).

Comparable results of ion products distribution at decomposition of HAN (95 wt.%) – water solution in presence of 1~3 wt.% activated carbon CRH-KOH at different heating rates (16–128 K/min) were shown in Fig. 9.

The distribution of product ion decomposition of HAN is presented in percentages, which were calculated using the signal intensities that derived by EI-MS method. Figure 9 shows the product ions with abundance greater than 2% of the total signal. Activated carbon CRH-KOH in investigated sample is influencing significantly on product ions distribution and as a consequence reducing the formation of NOx ions almost up to 30%.

The reduction of amount of gases NOx in the presence of activated carbons is a topic of many discussions for today. For example, Kaneko [23] has supposed that the adsorption of NO gases is occurred in activated carbon micropores. Also, Teng and Suuberg [24] suggested that the adsorption is caused by the transformation of NO into N_2 with surface oxides. Based on the review of recent researches on this problem, we tend to follow the mechanism which has been proposed by W.J. Zhang [25], where the physical adsorption pathway of NO gas is described. Finally, we suggest a perspective of activated carbon CRH-KOH as an agent for reducing of NOx compound emissions due to HAN decomposition.

4. Conclusions

According to the experimental studies, the obtained results showed that:

- The burning rate of HAN (95 wt.%) – water solution was measured in addition of four types of activated carbon. The burning rate of HAN (95 wt.%) – water solution have been jumped in presence of activated carbon CRH-KOH (until rb = 400 mm/sec at highest pressures 6 MPa). Also, it was shown that the linear burning rate of HAN may be high, even with low concentration of activated carbon.

- In the presence of activated carbons, there is observed a dramatic change of decomposition behaviour of HAN (95 wt.%) – water solution in comparison with the thermal decomposition of HAN (95 wt.%) – water solution alone. The thermal decomposition of hydroxylammonium nitrate (95 wt.%) – water solution admixed with activated carbon CRH-KOH shown the ability to trigger the decomposition at lower temperatures (86 °C versus 185 °C) in order to avoid or reduce the use of noble metals in future prospective.

- The results of EI-MS product ions analysis indicated that the addition of activated carbon allows to reduce significantly the amounts of NO*x* gases by 30 %. With the addition of activated carbon, a double stage thermal decomposition of pure HAN (95 wt.%) – water solution becomes single stage with a reduction of decomposition temperature by 40–45 °C. The usage of activated carbon additives is economically advantageous because it is a low-cost.

References

[1]. R. Amrousse, T. Katsumi, N. Itouyama, N. Azuma, H. Kagawa, K. Hatai, H. Ikeda, K. Hori, *Combust. Flame* 162 (2015) 2686–2692. DOI: 10.1016/j.combustflame.2015.03.026

[2]. R. Amroussea, K. Horia, W. Fetimi, K. Farhatc, *Appl. Catal. B* 127 (2012) 121–128. DOI: 10.1016/j.apcatb.2012.08.009

[3]. W.F. Oberle, G.P. Wren, Closed chamber combustion rates of liquid propellant 1846 conditioned ambient, hot and cold vulnerability testing of liquid propellant LGP 1846. Proc. 27th JANNAF Combustion Subcommittee Meeting, 557 (1990) 377–385.

[4]. W.F. Oberle, G.P. Wren, Burn Rates of LGP 1846 Conditioned Ambient, Hot, and Cold. Army Ballistic research laboratory, technical report no. BRL-TR-3287, 1991, USA (1991).

[5]. S.T. Jennings, Y. Chang, D. Koch, K.K. Kuo, Peculiar combustion characteristics of XM46 liquid propellant. Proc. 34th JANNAF Combustion Subcommittee Meeting, FL, USA. 1 (662) (1997) 321–331.

[6]. J.L. Sabourin, D.M. Dabbs, R.A. Yetter, F.L. Dryer and I.A. Aksay, *ACS Nano* 3 (12) (2009) 3945–3954. DOI: 10.1021/nn901006w

[7]. M. Atamanov, I. Noboru, T. Shotaro, R. Amrousse, M. Tulepov, A. Kerimkulova, M. Hobosyan, K. Hori, K. Martirosyan, Z. Mansurov, *Combust. Sci. Technol.* 188 (2016) 2003–2011. DOI: 10.1080/00102202.2016.1220143

[8]. M.K. Atamanov, I. Noboru, T. Shotaro, R. Amrousse, K. Hori, Y. Aliyev, Z.A. Mansurov. The process of combustion and thermal analysis system of ammonium nitrate and carbonized rice husk. Proc. VIII Int. Symp. "Combustion and plasmachemistry", Almaty, Kazakhstan (2015) p. 243–245.

[9]. V.V Barzykin, *Gorenie i plazmohimija* [Combustion and Plasmachemistry] 2 (4) (2004) 275–292 (in Russian).

[10]. B.N. Kondrikov, V.É. Annikov, V.Yu. Egorshev, L.T. De Luca, *Combust. Explo. Shock* 36 (2000) 135–145. DOI: 10.1007/BF02701522

[11]. T. Katsumi, H. Kodama, H. Shibamoto, J. Nakatsuka, K. Hasegawa, K. Kobayashi, H. Ogawa, N. Tsuboi, Sh. Sawai, K. Hori, *Int. J. Energ. Mater. Chem. Propuls.* 7 (2008) 123–137. DOI: 10.1615/IntJEnergeticMaterialsChemProp.v7.i2.30

[12]. T. Katsumi, R. Matsuda, T. Inoue, N. Tsuboi, H. Ogawa, Sh. Sawai, K. Hori , *Int. J. Energ. Mater. Chem. Propuls* 9 (2010) 219–231. DOI: 10.1615/IntJEnergeticMaterialsChemProp.v9.i3.30

[13]. Y. Qiu, Z. Wang, A.C. Owens, I. Kulaots, Y. Chen, A.B. Kane, R.H. Hurt. *Nanoscale* 6 (20) (2014) 11744–11755. DOI: 10.1039/c4nr03275f.

[14]. T.B. Brill, T.P. Russell, *Proc. SPIE.* 0872 (1988) 40–43. DOI: 10.1117/12.943751

[15]. Y.J. Lee, T.A. Litzinger, *Combust. Sci. Technol.* 141 (1999) 19–36. DOI: 10.1080/00102209908924180

[16]. Charlie Oommen, Santhosh Rajaraman, R. Arun Chandru and R. Rajeev, Catalytic Decomposition of Hydroxylammonium Nitrate Monopropellant. Int. Conf. Chemistry and Chemical Process IPCBEE, Singapore (2011) 205–209.

[17]. R. Amrousse, T. Katsumi, T. Sulaiman, B.R. Das, H. Kumagai, K. Maeda, K. Hori, *Inter. J. Energy Mater. Chem. Propul.* 11. (2012) 241–257. DOI: 10.1615/IntJEnergeticMaterialsChemProp.2012004978

[18]. M. Atamanov, K. Hori, R. Amrousse, A. Kerimkulova, J. Jandosov, Z. Mansurov. Effect of KOH-activated rice husk on thermal decomposition of hydroxylamine nitrate monopropellant. Proc. 9th Int. Seminar on flame structure, pp. 32, July 10-14, 2017, Novosibirsk, Russia.

[19]. M. Atamanov, K. Hori, E. Aliyev, R. Amrousse, Z. Mansurov. Experimental Investigations of Combustion Enhancement of HAN-Based Green Propellant with K_2CO_3–Activated Carbon. International Colloquium on the dynamics of explosion and reactive systems (1063), Boston, USA, 2017

[20]. Ya.B. Zel'dovich, P.Ya. Sadovnikov, D.A. Frank-Kamenetsky, Oxidation of nitrogen during combustion. Publishing house of the USSR academy of Sciences, Moscow, 1947. p. 145.

[21]. H.S. Lee, T.A. Litzinger, *Combust. Flame* 135 (2003) 151–169. DOI: 10.1016/S0010-2180(03)00157-3

[22]. A.P. Sanoop, R. Rajeev, B.K. George, *Thermochim. Acta* 606 (2015) 34–40. DOI: 10.1016/j.tca.2015.03.006

[23]. K. Kaneko, *Langmuir* 3 (1987) 357–363. DOI: 10.1021/la00075a014

[24]. H. Teng, E.M. Suuberg, *Ind. Eng. Chem. Res.* 32 (1993) 416–423. DOI: 10.1021/ie00015a004

[25]. W.J. Zhang, S. Rabiei, A. Bagreev, M. Zhuang, F. Rasouli, *Appl. Catal.* (2008) 63–71. DOI: 10.1016/j.apcatb.2008.02.003